

**Assessing the aerobic/anoxic enrichment efficiency at different C/N ratios  
Polyhydroxyalkanoate production from waste activated sludge**

Mineo, Antonio; van Loosdrecht, Mark M.C.; Mannina, Giorgio

**DOI**

[10.1016/j.watres.2024.122687](https://doi.org/10.1016/j.watres.2024.122687)

**Publication date**

2025

**Document Version**

Final published version

**Published in**

Water Research

**Citation (APA)**

Mineo, A., van Loosdrecht, M. M. C., & Mannina, G. (2025). Assessing the aerobic/anoxic enrichment efficiency at different C/N ratios: Polyhydroxyalkanoate production from waste activated sludge. *Water Research*, 268, Article 122687. <https://doi.org/10.1016/j.watres.2024.122687>

**Important note**

To cite this publication, please use the final published version (if applicable).  
Please check the document version above.

**Copyright**

Other than for strictly personal use, it is not permitted to download, forward or distribute the text or part of it, without the consent of the author(s) and/or copyright holder(s), unless the work is under an open content license such as Creative Commons.

**Takedown policy**

Please contact us and provide details if you believe this document breaches copyrights.  
We will remove access to the work immediately and investigate your claim.



# Assessing the aerobic/anoxic enrichment efficiency at different C/N ratios: polyhydroxyalkanoate production from waste activated sludge

Antonio Mineo<sup>a</sup>, Mark M.C. van Loosdrecht<sup>b</sup>, Giorgio Mannina<sup>a,\*</sup>

<sup>a</sup> Engineering Department, Palermo University, Viale delle Scienze ed. 8, Palermo 90128, Italy

<sup>b</sup> Department of Biotechnology, Delft University of Technology, Van der Maasweg 9, Delft 2629 HZ, the Netherlands

## ARTICLE INFO

### Keywords:

Bioplastic  
Biosolid management  
Greenhouse gas emission  
Resource recovery  
Wastewater

## ABSTRACT

Polyhydroxyalkanoates (PHA) can be produced using fermentation products of an excess sewage sludge fermentation process. An efficient method to enrich a PHA-producing community is an aerobic-feast/anoxic-famine enrichment strategy. The effect of different carbon to nitrogen (C/N) feed ratios of 1, 2 and 3.5 g COD/g N on the process performance was studied. The study was executed on a pilot plant scale using fermented waste activated sludge as the organic carbon source. The system's performance was monitored in terms of removing contaminants, producing PHA, and reducing N<sub>2</sub>O emissions. The results indicated that a lower C/N ratio results in lower PHA production, with PHA content in the sludge of 20, 24 and 36 % w/w for C/N ratios of 1, 2 and 3.5 g COD/g N, respectively. At the lowest C/N ratio, the highest nitrite accumulation rate (77 %), nitrification efficiency (89 %) and denitrification efficiency (89 %) were observed, but the N<sub>2</sub>O production was also the highest (0.77 mg N<sub>2</sub>O-N/L). The long-term comprehensive monitoring carried out in this study revealed high carbon and ammonia removal efficiencies (never below 80 %) despite the C/N shifts and high COD and ammonia concentrations. At the same time, the system showed relatively low PHA production and high environmental impact in terms of high gaseous N<sub>2</sub>O emission. These findings question the sustainability of the aerobic-feast/anoxic-famine enrichment strategy for PHA production in full-scale plants.

## 1. Introduction

Polyhydroxyalkanoates (PHAs) production involves microorganisms able to convert organic waste from wastewater streams into carbon storage compounds, such as PHA. The process, based on mixed microbial cultures, is composed of three steps: i) organic waste fermentation to produce volatile fatty acids (VFA), used as a carbon source to produce PHA; ii) enrichment of the microorganisms able to produce PHA; iii) accumulation of intracellular PHA (Bugnicourt et al., 2014; Mannina et al., 2020). Despite being a promising way to achieve sustainable plastic production and waste reduction, its large-scale implementation

in wastewater treatment plants (WWTPs) is still in its infancy (Guleria et al., 2022; Varghese et al., 2022).

Several strategies have been developed over the years to implement a PHA production process in the wastewater treatment operation, using mixed microbial cultures (MMCs) under feast and famine conditions to select microorganisms capable of accumulating PHA efficiently (Frigon et al., 2006; Johnson et al., 2009). This strategy, known as Aerobic Dynamic Feeding (ADF), capitalizes on the metabolic versatility of MMCs, enabling the utilization of a wide range of substrates present in wastewater, adopting the transient limitation of carbon source as a driving force to enrich specific microbial cultures able to produce PHA

**Abbreviations:** ADF, Aerobic Dynamic Feeding; AE/AN, Aerobic/Anoxic; AOB, Ammonia Oxidizing Bacteria; BOD, Biochemical Oxygen Demand; C/N, Carbon to Nitrogen ratio; COD, Chemical Oxygen Demand; DO, Dissolved Oxygen; EPS, Extra Polymeric Substances; F/M, Food to Microorganism ratio; GC, Gas Chromatograph; GHG, Greenhouse Gas; HRT, Hydraulic Retention Time; MMCs, Mixed Microbial Cultures; N-SBR, Nitrification Sequencing Batch Reactor; NAR, Nitrite Accumulation Rate; NH<sub>4</sub>-N, Ammonium; NLR, Nitrogen Loading Rate; NOB, Nitrite Oxidizing Bacteria; NO<sub>2</sub>-N, Nitrite; NO<sub>3</sub>-N, Nitrate; N<sub>2</sub>O, Nitrous Oxide; OLR, Organic Loading Rate; PHA, Polyhydroxyalkanoate; PHB, Polyhydroxybutyrate; PHV, Polyhydroxyvalerate; PO<sub>4</sub>-P, Phosphate (orthophosphate); SBR, Sequencing Batch Reactor; S-SBR, Selection Sequencing Batch Reactor; SMP, Soluble Microbial Products; SRT, Sludge Retention Time; T, Temperature; TCOD, Total Chemical Oxygen Demand; TSS, Total Suspended Solids; UF, Ultrafiltration; VFA, Volatile Fatty Acid; VSS, Volatile Suspended Solids; WAS, Waste Activated Sludge; WWTP, Wastewater Treatment Plant; WRRF, Water Resource Recovery Facility.

\* Corresponding author.

E-mail address: [giorgio.mannina@unipa.it](mailto:giorgio.mannina@unipa.it) (G. Mannina).

<https://doi.org/10.1016/j.watres.2024.122687>

Received 6 August 2024; Received in revised form 5 October 2024; Accepted 22 October 2024

Available online 22 October 2024

0043-1354/© 2024 The Author(s). Published by Elsevier Ltd. This is an open access article under the CC BY license (<http://creativecommons.org/licenses/by/4.0/>).

(Jelmer et al., 2018; Reis et al., 2003; Valentino et al., 2015). In the last years, many studies have focused on assessing the effect of different substrates (Valentino et al., 2017) and operational parameters (Sabapathy et al., 2020), also successfully demonstrating its effectiveness at a pilot scale (Bengtsson et al., 2017). In recent years, the aerobic/anoxic (AE/AN) enrichment (Kourmentza et al., 2017) was implemented by N. Frison et al. (2015a, N. 2015b) and Basset et al. (2016) as a novel scheme to couple the nitrification/denitrification with PHA production. The process is based on aerobic feast and anoxic famine, where nitrate and nitrite produced during the feast are used as electron acceptors, taking advantage of the PHA produced as a carbon source to perform denitrification. While Basset et al. (2016) proposed the process with a single enrichment reactor, Frison et al. (2015) used a nitrification reactor upstream of the enrichment reactor, proving its benefit in the system performance and PHA production which has been successfully validated in long-term operation (Conca et al., 2020). Still, in recent years, literature lacks further approach and consideration towards this enrichment strategy, considering the overall system performance rather than only the PHA produced (Liu et al., 2023).

Many parameters influencing PHA production with different enrichment strategies have been evaluated, such as organic loading rate, substrate used, pH, cycle length, etc. (Puyol et al., 2017). However, there is a lack of the influence of the C/N ratio, which can influence nitrification and nitrogen removal in the biological nitrogen removal processes (Mannina et al., 2016a) and can be considered a key parameter in the PHA production process (Johnson et al., 2010a, 2010b). Also, as reported in several studies regarding the greenhouse gas (GHG) emissions in WWTPs, the C/N ratio highly affects the nitrous oxide (N<sub>2</sub>O) emissions, thus affecting the carbon footprint and, therefore, the sustainability of the process (Gruber et al., 2021; Rodriguez-Caballero et al., 2015). The literature lacks information regarding the sustainability of the PHA production process based on contaminants removal, amount of PHA produced and carbon footprint assessment.

This study is focused on the evaluation of the PHA production from VFA produced by sewage sludge fermentation by a culture enrichment operated under aerobic and anoxic conditions, applying the AE/AN enrichment strategy with a nitrification reactor as described by Frison et al. (2015). The influence of three COD/N ratios (3.5, 2 and 1 g COD/g N) has been evaluated during the long-term pilot plant operation by applying a comprehensive, holistic approach considering the system performance in contaminants removal, PHA production capacity and N<sub>2</sub>O emission, both in gaseous and liquid form.

## 2. Materials and methods

### 2.1. Experimental layout

The experiments were carried out at the Water Resource Recovery Facility (WRRF) of Palermo University (Mannina et al., 2021). The PHA production line is located in the pilot plant hall and is fed by the waste activated sludge produced by the main stream. The PHA line comprises a fermenter with a working volume of 200 L equipped with an ultra-filtration (UF) unit and two sequencing batch reactors (SBR) working in series. The nitrification SBR (N-SBR) aims to produce a nitrites rich effluent (working volume of 30 L) by partially oxidizing the ammonia in the fermented sludge's liquid. The selection SBR (S-SBR) aims to enrich the PHA producers' microorganisms within the microbial cultures with a feast-famine cycle by applying the AE/AN enrichment strategy (working volume of 30 L). At the start of the feast phase, the reactor is fed with the VFAs contained in the fermented sludge's liquid; at the beginning of the famine phase, it is fed with the N-SBR effluent rich in nitrites/nitrates. At the end of the selection process, the enriched biomass was subjected to batch scale accumulation by adopting home-made software (Mineo et al., 2023). The fermenter, N-SBR and S-SBR biomass inoculum was the waste sewage sludge withdrawn from the aerobic reactor of the water treatment line of the pilot plant hall

(Mannina et al., 2021). The experiments were conducted over three experimental periods where the C/N ratio (g COD/g N) both in the N-SBR and S-SBR varied as follows: i) period I – COD/N 3.5; ii) period II – COD/N 2; iii) period III – COD/N 1.

Fig. 1

### 2.2. Sewage sludge fermentation

Each acidogenic fermentation had a hydraulic retention time (HRT) and sludge retention time (SRT) of 5 days. The fermenter was a Continuous Stirred Tank Reactor with liquid and gas sampling points (total volume of 225 L). The fermenter was coupled to an ultra-filtration (UF) unit (total volume of 40 L) equipped with a hollow fibre membrane of polyvinylidene fluoride with 0.03- $\mu$ m porosity and 1.4-m<sup>2</sup> surface area. At the end of the fermentation, the sludge was pumped to the UF unit, where it was filtered to recover VFA rich liquid. pH and temperature were monitored but not controlled during the acidogenic fermentation, and no pre-treatment was performed before the fermentation. The inoculum sewage sludge features are reported in Table 1, while the fermentation's operational parameters are reported in Table 2.

### 2.3. Nitrification and selection SBR

Liquid rich VFA obtained after the filtration was used to feed the N-SBR and S-SBR. The N-SBR cycle was based partially on the aerobic reaction to partially oxidize ammonia to nitrite. The cycle lasted  $3.5 \pm 0.5$  h, depending on the conditions, and it was composed of feeding, reaction, settling and effluent discharge. The effluent was stored in a tank and used to feed at the start of the famine phase in the S-SBR. The reactor was operated with an HRT of 1 day and an average SRT of  $5.8 \pm 0.4$  days. The main operational conditions for N-SBR are reported in Table 3. The S-SBR cycle was based on the aerobic feast-anoxic famine strategy. It was composed of feeding, aerobic reaction, feeding from N-SBR, anoxic reaction, settling and effluent discharge. Overall, the cycle lasted for  $10 \pm 1$  h, where the aerobic feast accounted for 1 to 3 h, depending on the enrichment progress. pH, dissolved oxygen (DO) and temperature (T) were continuously monitored using two probes installed inside the reactors. The S-SBR's HRT was set at two days, while the average SRT was  $7.7 \pm 3.1$  days. The operational conditions for the S-SBR are reported in Table 4.

### 2.4. PHA accumulation

The PHA accumulation was run in fed batch mode with two 1.5 L reactors. Briefly, 3 L of mixed liquor was withdrawn from the S-SBR and after settling, 2 L of supernatant were removed. Biomass was washed twice with tap water, and the supernatant was removed each time to ensure no carbon source was available. Finally, the biomass was left aerated overnight to achieve the endogenous conditions before starting the accumulation. Subsequently, the accumulation was performed using the fermented sludge liquid as a carbon source and the DO as a parameter to run the accumulation automatically, as Mineo et al. (2023) reported. When the maximum volume inside the reactor was reached, the biomass was left settling for 20 minutes, and the supernatant was removed. The accumulation was performed in duplicate for each experimental period for ten days.

### 2.5. Analytical methods

The fermentation process was monitored three times per week by analysing soluble chemical oxygen demand (sCOD), VFA, ammonium (NH<sub>4</sub><sup>+</sup>-N) and phosphate (PO<sub>4</sub><sup>3-</sup>-P). Total chemical oxygen demand (TCOD), extra polymeric substances (EPS), soluble microbial products (SMP), total and volatile suspended solids (TSS, VSS) were monitored at the start and the end of the fermentation process.

S-SBR and N-SBR were monitored twice weekly by sampling the

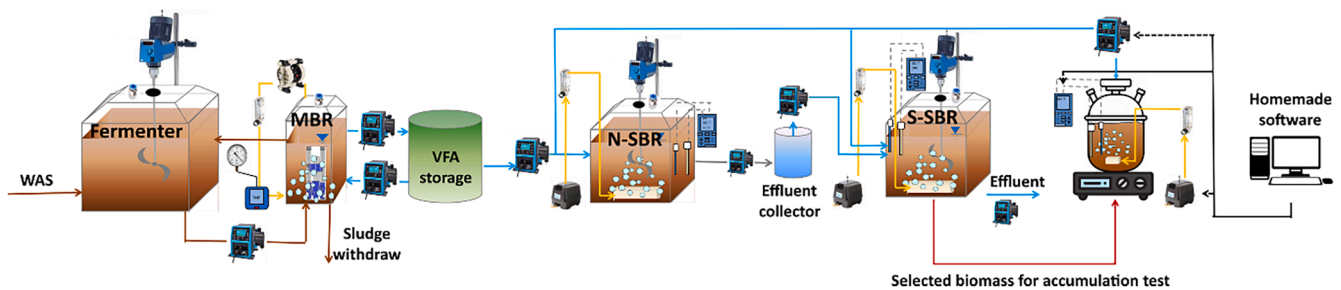


Fig. 1. Layout of the PHA production line.

**Table 1**  
Inoculum sewage sludge features.

Weeks	F/M kg BOD kg SS <sup>-1</sup> day <sup>-1</sup>	SRT Days	EPS mg g <sup>-1</sup> VSS	SMP mg g <sup>-1</sup> VSS
1	0.25	20.0	107.47	1.21
2	0.01	5.0	142.37	76.29
3	0.02	7.0	156.44	51.37
4	0.11	10.2	232.37	0
5	0.12	4.8	320.33	120.24
6	0.05	4.8	101.52	35.69
7	0.05	4.5	133.15	22.34
8	0.05	12.6	107.84	1.3
9	0.28	9.7	154.89	0.35
10	0.28	11.3	149.82	0
11	0.17	10.5	202.35	0.65
12	0.23	13.1	168.92	5.14

influent, mixed liquor inside the reactor and effluent. sCOD, NH<sub>4</sub><sup>+</sup>-N, PO<sub>4</sub><sup>3-</sup>-P, nitrate (NO<sub>3</sub>-N) and nitrite (NO<sub>2</sub>-N) were monitored in the influent and effluent. Mixed liquor samples were also collected to determine TSS, VSS, EPS, SMP, and dissolved N<sub>2</sub>O (Mannina et al., 2018a). Dissolved N<sub>2</sub>O was also continuously monitored during the feast/famine cycle of the S-SBR by a micro-sensor (Unisense

**Table 2**  
Fermentation parameters.

Weeks	Total Suspended Solids (TSS) g/L	Volatile Suspended Solids (VSS) g/L	Starting pH – Ending pH	Temperature °C
1	3.3	1.4	7.2 – 6.6	12.5 ± 2.1
2	2.9	1.3	7.1 – 6.3	11.8 ± 1.2
3	3.5	2.1	7.5 – 6.7	12.3 ± 3.1
4	3.1	1.7	6.9 – 6.2	11.4 ± 1.2
5	2.7	1.1	7.1 – 6.8	13.2 ± 1.6
6	3.9	1.8	7.6 – 6.4	14.5 ± 1.2
7	3.1	1.3	7.5 – 6.2	14.1 ± 2.4
8	3.4	1.6	7.4 – 6.5	15.3 ± 2.7
9	3.5	1.9	7.1 – 6.3	16.4 ± 2.4
10	3.6	2.1	6.9 – 6.2	17.1 ± 1.8
11	2.8	1.1	7.1 – 6.4	18.1 ± 0.9
12	3.7	1.8	6.8 – 6.2	18.5 ± 1.7

**Table 3**  
Operational conditions of the nitrification SBR.

Parameter	U.M.	Period		
		I	II	III
F/M	kg BOD kg SS <sup>-1</sup> d <sup>-1</sup>	0.03 ± 0.01	0.03 ± 0.02	0.07 ± 0.02
vOLR	kg COD m <sup>-3</sup> d <sup>-1</sup>	0.05 ± 0.03	0.06 ± 0.01	0.14 ± 0.01
vNLR	kg N m <sup>-3</sup> d <sup>-1</sup>	0.02 ± 0.01	0.03 ± 0.01	0.13 ± 0.02
EPS	mg g <sup>-1</sup> VSS	183.27 ± 14.7	191.89 ± 14.70	300.92 ± 63.49
SMP	mg g <sup>-1</sup> VSS	34.46 ± 17.32	8.52 ± 3.91	10.09 ± 6.47

Environment A/S, Denmark). Gaseous N<sub>2</sub>O samples were collected by directly sampling the headspace volume of the N-SBR and S-SBR (Mannina et al., 2018a).

During the accumulation, mixed liquor samples were collected daily to determine the PHA as the sum of the polyhydroxy butyrate (PHB) and polyhydroxy valerate (PHV) concentrations as well as TSS and VSS (Conca et al., 2020). sCOD, TCOD, NH<sub>4</sub><sup>+</sup>-N, PO<sub>4</sub><sup>3-</sup>-P, NO<sub>3</sub>-N, NO<sub>2</sub>-N, EPS, SMP, TSS and VSS were analysed using standard methods (Rice et al., 2012). Based on the parameter, chemical analyses were carried out on unfiltered or filtered samples (0.45 µm), analysed through UV-VIS spectroscopy methods. EPS and SMP were extracted using thermal extraction (Cosenza et al., 2013). The protein and carbohydrate content were analysed according to Lowry's and DuBois' methods, respectively (DuBois et al., 1956; Lowry et al., 1951). TSS are analysed following the 105 °C dry method, while the VSS are analysed by igniting at 550 °C the residue of the TSS analysis (Symons and Morey, 1941). VFA concentrations were evaluated, as reported by Montiel-Jarillo et al. (2021), by using a Gas Chromatograph (GC) (Agilent 8860) with a flame ionization detector (FID) and a DB FFAA column (30 m x 0.25 mm x 0.25 µm). PHB and PHV concentrations were measured using a GC equipped with an FID and a Restek Stabilwax column (30 m x 0.53 mm x 1.00 µm) (Mannina et al., 2019). Gaseous and dissolved N<sub>2</sub>O concentrations were measured, as reported by Mannina et al. (2018b), by using a GC with an electron capture detector and a Porapak-Q 80/100 mesh column (6 ft x 1/8 in x 2.1 mm).

## 2.6. Calculations

The PHA concentration was expressed as a weight ratio based on the gram of PHA per gram of VSS (g PHA/g VSS) (Conca et al., 2020). PHA productivity was defined as the gram of PHA produced daily (g PHA/day).

The Nitrite Accumulation Rate (NAR) was calculated as reported by Kowal et al. (2022):

$$NAR (\%) = \frac{(NO_2 - N_{out})}{(NO_2 - N_{out} + NO_3 - N_{out})} * 100 \quad (\text{Eq. 1})$$

The nitrogen mass balance was calculated as reported by Mannina

**Table 4**  
Operational conditions of the selection SBR.

Parameter	U.M.	Period		
		I	II	III
F/M	kg BOD kg SS <sup>-1</sup> d <sup>-1</sup>	0.03 ± 0.01	0.03 ± 0.01	0.06 ± 0.02
vOLR	kg COD m <sup>-3</sup> d <sup>-1</sup>	0.08 ± 0.05	0.10 ± 0.03	0.20 ± 0.01
vNLR	kg N m <sup>-3</sup> d <sup>-1</sup>	0.03 ± 0.02	0.05 ± 0.01	0.19 ± 0.03
COD <sub>SOL</sub> /NO <sub>x</sub> -N	g COD g <sup>-1</sup> NO <sub>x</sub> -N	22.69 ± 9.91	19.34 ± 8.32	14.06 ± 1.89
EPS	mg g <sup>-1</sup> VSS	179.16 ± 59.08	214.40 ± 6.58	296.82 ± 34.04
SMP	mg g <sup>-1</sup> VSS	19.25 ± 25.48	8.69 ± 7.72	11.93 ± 2.45

et al. (2016b):

$$N_{nit} = \frac{(NH_4^+ - N_{in}) - (NH_4^+ - N_{out}) - (N_{metabolic})}{(NH_4^+ - N_{in}) - (N_{metabolic})} \quad (\text{Eq. 2})$$

$$N_{denit} = \frac{(NH_4^+ - N_{in}) + (NO_x - N_{in}) - (NH_4^+ - N_{out}) - (N_{metabolic}) - (NO_x - N_{out})}{(NH_4^+ - N_{in}) + (NO_x - N_{in}) - (N_{metabolic})} \quad (\text{Eq. 3})$$

where  $N_{metabolic}$  is the 5 % of the sCOD removed.

The  $N_2O$  emission factor was calculated as reported by Eq. 4 (Tsuneda et al., 2005):

$$EF_{N_2O} = \frac{\frac{N_2O - N_g}{HRT_{hs}} + \frac{N_2O - N_d}{HRT}}{TN} \quad (\text{Eq. 4})$$

Where  $N_2O - N_g$  is the gaseous  $N_2O$  concentration,  $N_2O - N_d$  is the dissolved  $N_2O$  concentration, HRT is the PHA line hydraulic retention time,  $HRT_{hs}$  is the retention time in the reactor headspace, and TN is the concentration of total nitrogen in the influent.

### 3. Results and discussion

#### 3.1. Acidogenic fermentation performance

Sewage sludge fermentation was performed to obtain a VFA rich substrate for N-SBR, S-SBR and the accumulation batch reactors. The fermentation was carried out for 12 weeks, divided into four weeks per period (Fig. 2a). During the first five weeks, the produced sCOD showed an increasing trend, reaching the peak in week 5 (545.9 mg/L) starting from 200.3 mg/L in week 1. Weeks 6 to 8 were characterized by a low sCOD production (180, 192 and 284 mg/L for weeks 6, 7 and 8, respectively) and an average VFA/sCOD ratio of  $0.31 \pm 0.03$ , lower than the previous weeks. The highest amount of VFA was achieved during the third and last period. During weeks 9 to 12, sCOD was 572, 556.9, 617.6 and 594.2, with a VFA/sCOD of 0.42, 0.44, 0.45 and 0.48 for weeks 9, 10, 11 and 12, respectively. The nutrients release reported in Fig. 2b shows an almost constant ammonium concentration at the peak of the fermentation process over the three experimental periods ( $81.8 \pm 10.7$ ,  $88.9 \pm 9.3$  and  $83.8 \pm 7.8$  mg N/L for period I, II and III, respectively). Small changes were noticed regarding the phosphate concentration, achieving  $29.7 \pm 17.8$ ,  $20.9 \pm 5.6$  and  $18.9 \pm 2.4$  mg P/L for period I, II and III, respectively. The increasing trend in sCOD during the first five weeks may be related to increased EPS in the sludge (Table 1), indicating a growing amount of organics available (Li et al., 2023; She et al., 2020). Still, this conflicts with the constant ammonium concentration in the effluent, indicating no improvement in the organics' hydrolysis (Ye et al., 2020; Zhang and Chen, 2009). During the period I and II, characterized by a low sCOD production, the highest VFA were obtained in week 5 with a VFA/sCOD ratio of 0.37 followed by weeks 4 and 3 with a VFA/sCOD ratio of 0.41 and 0.33, respectively. This result may be due to the different sewage sludge features and operational conditions. Low SRT and medium-high F/M characterized the sludge adopted in week 5 compared to the other in the first two periods. Sludge with low SRT and high F/M is less mineralised, indicating enhanced biological activity of the microorganism, as shown by the higher concentration of EPS and SMP (Geyik and Çeçen, 2015; Huang et al., 2022). As previously discussed for the first five weeks, the EPS and SMP concentrations cannot be considered the only factor influencing the fermentation process for period III. Indeed, the highest F/M ratios were recorded for the sludge from weeks 9 to 12, ranging from 0.17 to 0.28 (Table 1), indicating a less mineralised sludge that can be more easily degraded.

Fig. 2c shows the VFA distribution over the 12 weeks of acidogenic fermentation. Overall, acetic acid was the main VFA measured during the entire period, with an average share of  $72.18 \pm 13.16$  %, followed by propionic ( $13.8 \pm 11.6$  %) and butyric acid ( $14.0 \pm 13.2$  %), while the other VFA accounted for less than 0.1 %. During the first four weeks, acetic acid accounted for  $81.9 \pm 6.3$  %, the highest share measured over

the entire period. Butyric acid was also abundant in the first period ( $12.67 \pm 10.42$  %), with the highest share registered in the first ( $23.8$  %) and fourth week ( $17.9$  %). As previously stated in literature (Mannina and Mineo, 2023; Ucisik and Henze, 2008), the butyric acid may be related to the SRT adopted in the plant from where the sludge was withdrawn. The SRT effect is also confirmed for weeks 8, 10, 11 and 12, where the butyric acid accounted for 22.2, 34.8, 33.8 and 19.1 % of the

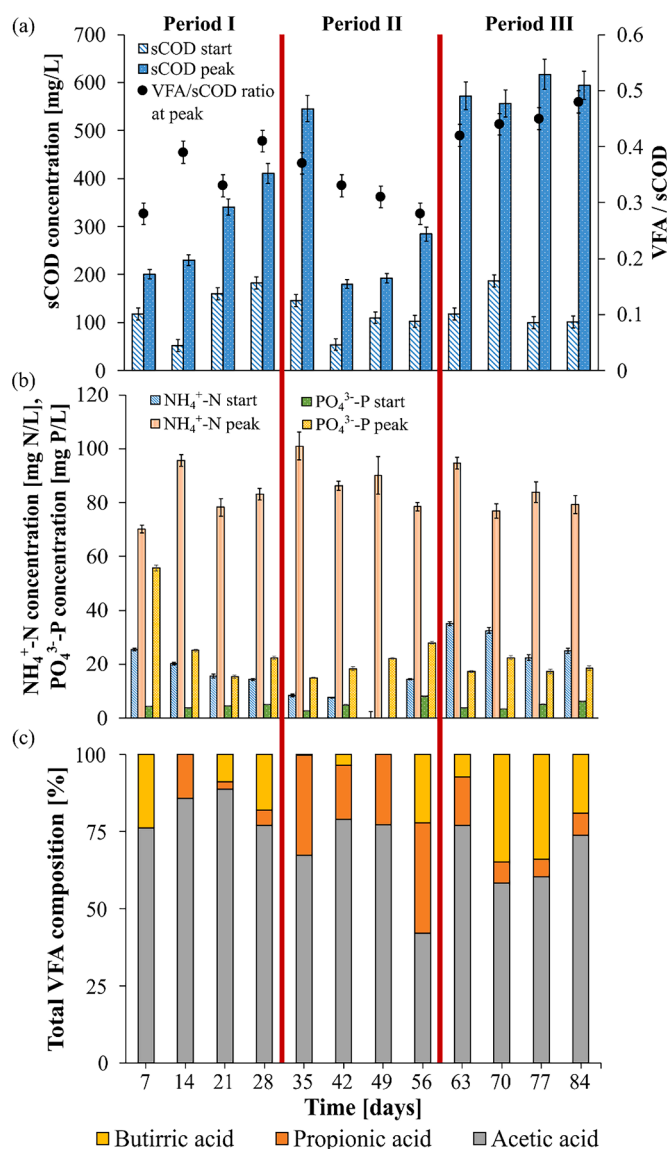


Fig. 2. VFA and sCOD production (a), ammonium and phosphate release (b) and VFA composition (c) obtained during the fermentation.

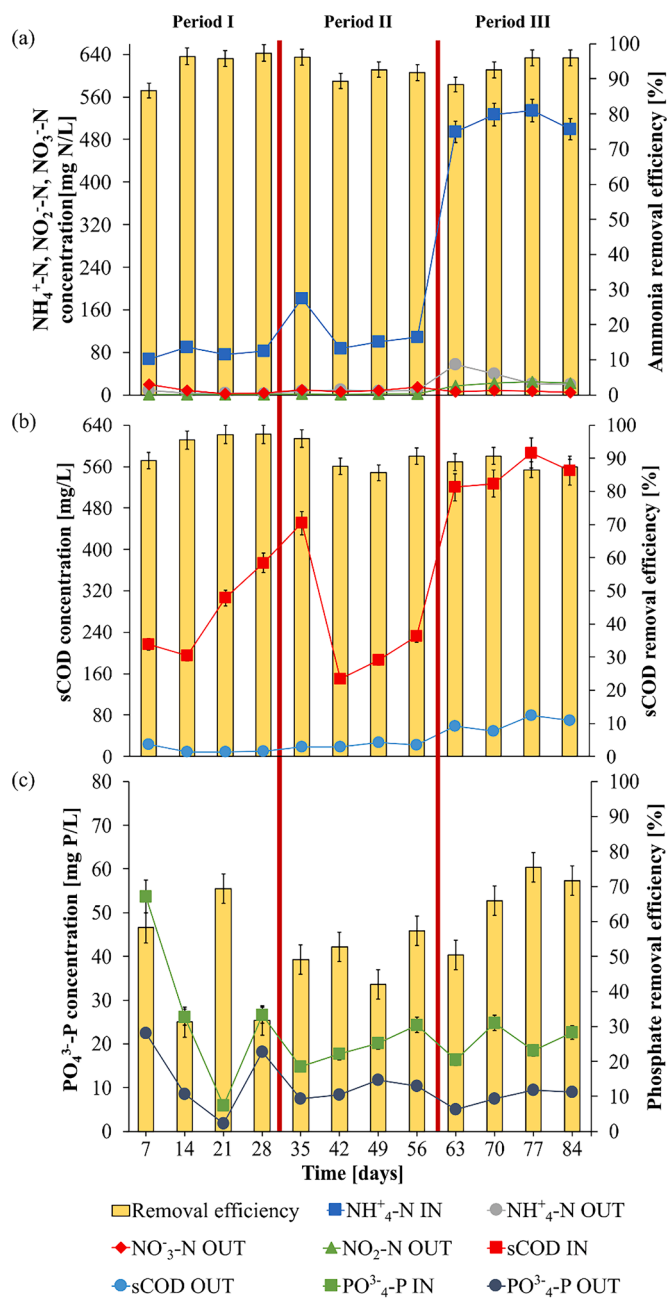


Fig. 3. Ammonium (a), sCOD (b) and phosphate (c) removal efficiency for N-SBR.

total VFA, respectively. Overall, the highest butyric acid concentration was measured for sludge with a relatively high F/M ratio (higher than 0.16 kg BOD kg SS<sup>-1</sup> day<sup>-1</sup>) and high SRT (higher than 10 days). Propionic acid was more abundant during the second period (weeks 5 to 8), with an average share of 27.1 ± 8.5 %. The highest propionic acid production occurred for the less performant sludge in terms of sCOD production, especially in week 8, where a high SRT but low F/M were registered (Chen et al., 2021; Wu et al., 2023).

### 3.2. Contaminants removal

Ammonia, sCOD, and phosphate removal efficiencies are reported in Figs. 3 and 4 for N-SBR and S-SBR, respectively. The effluent nitrite and nitrate concentrations are included in Figs. 3a and 4a to calculate nitrification and denitrification efficiency.

In terms of nitrogen removal, the first period was characterized by

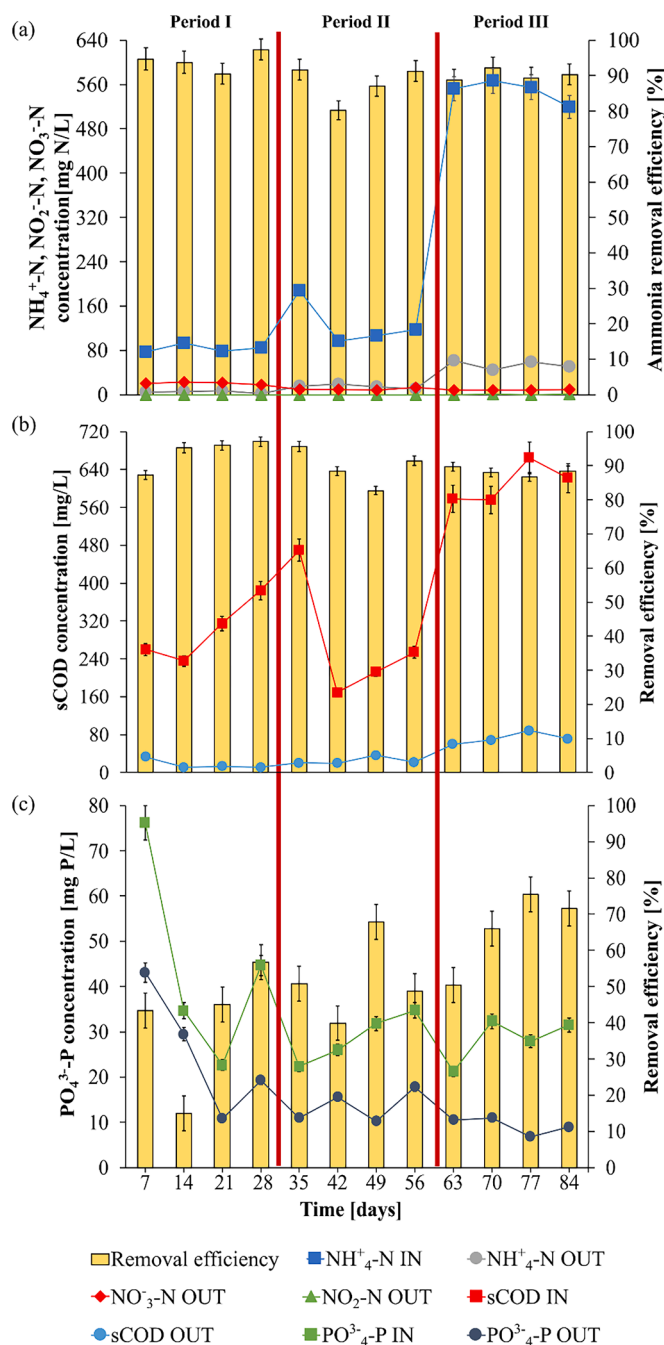


Fig. 4. Ammonium (a), sCOD (b) and phosphate (c) removal efficiency for S-SBR.

high ammonium removal efficiency (93.4 % and 93.9 % for N-SBR and S-SBR, respectively), high nitrification efficiency for N-SBR (93.4 %) and relatively high denitrification for S-SBR (71.2 %). The low denitrification in S-SBR was probably due to the moderate C/N ratio (3.5 g COD/g N) and low sCOD influent concentration, which can negatively affect heterotrophic biomass (Wang et al., 2021). Still, despite the high nitrification and ammonium removal efficiency for N-SBR, the NAR accounted only for 13.6 %. The low NAR may be related to the low influent ammonium concentration during period I, affecting the reactor's free ammonia concentration (Conca et al., 2020). Indeed, low free ammonia concentration can negatively affect Ammonia Oxidizing Bacteria (AOB) while favouring Nitrite Oxidizing Bacteria (NOB), thus achieving high nitrification but low NAR (Fu et al., 2009). As for period II (2 g COD/g N), the influent ammonium concentration did not change

significantly, leading to 16.6 % NAR and 89.7 % nitrification efficiency in the N-SBR. Also, no significant difference in ammonium removal was registered for N-SBR (89.7 %) and S-SBR (83.3 %). In comparison, a slight increase in denitrification for S-SBR led to an efficiency of 75 %, mainly due to the lower C/N ratio. The sharp increase of influent sCOD concentration during the last period and the lowest C/N ratio (1 g COD/g N) positively affected denitrification efficiency for S-SBR up to 83 %. On the other hand, N-SBR nitrification was not influenced (89 %), the same as ammonium removal efficiency (89 %), while the NAR reached 77 %. The high influent sCOD concentration and the low C/N ratio generated a high free ammonia concentration inside the reactors, thus inhibiting NOB in the N-SBR (Basset et al., 2016). The higher nitrite load for the S-SBR, coupled with a low C/N ratio, also favoured denitrification efficiency (Fu et al., 2009). Regarding nitrogen removal, the low C/N ratio (1 g COD/g N) proved to be the best condition for the AE/AN enrichment to achieve high ammonium removal, both in the N-SBR and S-SBR, and high nitrification/denitrification efficiency and nitrite production.

During the first period, characterized by a C/N ratio of 3.5 g COD/g N, a high sCOD removal efficiency was achieved for N-SBR and S-SBR (94.2 % and 94.0 % for N-SBR and S-SBR, respectively). A slight decrease in period II (C/N ratio of 2 g COD/g N) was registered, achieving 86.2 % for N-SBR and 87.3 % for S-SBR. Despite a lower C/N ratio influencing the biological activity (Mannina et al., 2016a), sCOD removal was above 85 % for both reactors. This may be related to the lower sCOD influent concentration during period II, which may have balanced the negative effect of the lower C/N ratio on both systems performance. During period III (C/N ratio of 1 g COD/g N), sCOD removal efficiency accounted for 82.1 % and 81.8 % for N-SBR and S-SBR, respectively. Despite being negatively affected by a lower C/N ratio and higher influent sCOD concentration, sCOD removal efficiency maintained above 80 % for both N-SBR and S-SBR, indicating excellent biological activity. During the last period, the biomass was subjected to influent wastewater with higher organic concentrations and a higher VFA/sCOD ratio compared to periods I and II. This may also suggest that despite the sCOD increase,  $45.06 \pm 0.02$  % of soluble organics were VFA, which are more easily consumed by PHA producers (Albuquerque et al., 2013; Liu et al., 2023).

During the first period, the phosphate removal efficiency accounted for 52.7 % and 41.8 % for N-SBR and S-SBR, respectively. The low removal efficiency is mainly due to the high nitrate concentration in N-SBR and low denitrification in S-SBR, which led to low P removal (Mulkerrins et al., 2004). The phosphate removal efficiency during period II was 50.3 % and 51.8 % for N-SBR and S-SBR, respectively. In the last period, the increased denitrification activity in S-SBR positively affected phosphate removal, achieving 65.9 %, the highest value registered in the experimental period. As for S-SBR, N-SBR was positively affected by the lower C/N ratio (1 g COD/g N), achieving 62.2 % phosphate removal efficiency.

### 3.3. PHA production

Despite the similarities in influent characteristics between the N-SBR and S-SBR systems, Basset et al. (2016) and Frison et al. (2015) utilized differing C/N ratios during the PHA accumulation phase. Specifically, substrate feeding reached around 1 g COD/L peaks during accumulation to enhance PHA production. In this study, the same influent and C/N ratio was consistently applied across the N-SBR, S-SBR and accumulation batch reactors to explore the effectiveness of employing the AE/AN enrichment as a selective strategy for treating nitrogen-rich influents. Once the steady state was achieved in the S-SBR, the biomass performed the PHA accumulation for ten days. Fig. 5 shows the PHA concentration and PHA productivity achieved for the three periods. Period I achieved the highest amount of PHA (Fig. 5a), reaching 0.36 g PHA/g VSS, with a PHV share of 8.3 % (0.33 and 0.03 g/g VSS of PHB and PHV, respectively). PHA productivity reached a peak on the first day (3.97 g

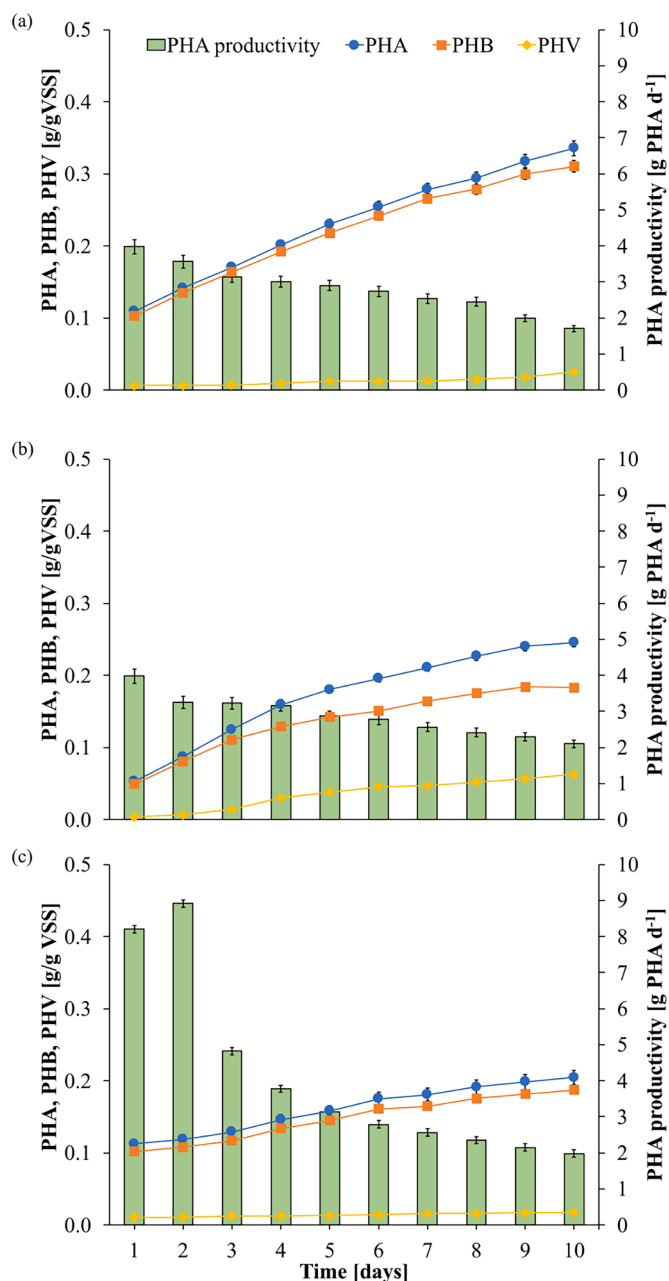


Fig. 5. Amount of PHB and PHV produced and PHA productivity monitored during the batch scale accumulations for period I (a), II (b) and III (c).

PHA/day), confirming the trend for biomass selected with low OLR (Isern-Cazorla et al., 2023). In period II (Fig. 5b), PHA accounted for 0.24 g PHA/g VSS, with a PHV share of 25 % (0.18 and 0.06 g/g VSS of PHB and PHV, respectively). The higher PHV share was due to the higher propionic acid share in the fermented liquid, as discussed in 3.1 (Albuquerque et al., 2011; Jab Chung et al., 1997). As for period I, PHA productivity reached a peak on the first day (3.97 g PHA/day) due to the similar OLR. Therefore, the PHA concentration difference is related to the C/N ratio rated compared to the OLR. The higher C/N ratio resulted in favourable conditions for biomass growth than PHA accumulation. Indeed, as stated in the literature, nitrogen deficiency is a key element in enhancing the amount of PHA produced (Cui et al., 2017). This result is also proved by the increased EPS concentration in period II compared to period I (Table 4), thus proving a biological activity more oriented towards growth (Chen et al., 2016; Yang et al., 2022). The same trend is noticeable in Fig. 5c, where the period III accumulation is reported. The

PHA produced was lower than in period II, reaching 0.20 g PHA/g VSS, with the lowest PHV share of 5 % (0.19 and 0.01 g/g VSS of PHB and PHV, respectively). The lower PHV production is related to the low propionic acid and highest butyric acid concentration of period III fermented liquid. Butyric acid concentration enhanced PHB production, thus reducing the PHV share despite a higher propionic acid concentration than in period I, where the highest PHV share was achieved. The PHA productivity reached the peak of 8.91 g PHA/day on the second day of accumulation, which was the highest value during the entire experimental period. This value and the day it reached is related to the higher OLR during the biomass selection. As previously reported (Mineo et al., 2023), if a higher OLR is adopted during the enrichment step, it will result in an overall higher but slower PHA productivity during the accumulation, compared to the lower OLR. Despite the highest OLR, the PHA concentration was the lowest of the entire experimental period, due to the lower C/N ratio adopted, as previously discussed for period II.

### 3.4. N<sub>2</sub>O emission

Fig. 6a reports the N<sub>2</sub>O emission in gaseous and liquid forms for N-SBR and S-SBR. S-SBR gaseous and liquid samples reported in the figure are an average based on both gaseous and liquid samples collected during the aerobic feast and anoxic famine phase. Over the entire experimental period, the N-SBR was the highest contributor towards N<sub>2</sub>O emission. In the first period (C/N 3.5 g COD/g N), the average N<sub>2</sub>O concentration was 0.41 mg N<sub>2</sub>O-N/L in the reactor headspace and 0.13 mg N<sub>2</sub>O-N/L in the mixed liquor for the N-SBR and 0.28 mg N<sub>2</sub>O-N/L and 0.16 mg N<sub>2</sub>O-N/L for the S-SBR, respectively. period I S-SBR N<sub>2</sub>O emissions are comparable to those reported in the literature for S-SBR where a different selection strategy is adopted, namely ADF (Mannina and Mineo, 2023). In the ADF S-SBR, an average N<sub>2</sub>O emission of 0.25 mg N<sub>2</sub>O-N/L and 0.14 mg N<sub>2</sub>O-N/L was achieved in gaseous and liquid form, respectively. The influent ammonium concentrations were comparable between the two cases (79.96 mg NH<sub>4</sub><sup>+</sup>-N/L for ADF and 82.13 mg NH<sub>4</sub><sup>+</sup>-N/L for period I) as well as the C/N ratio (3.71 g COD/g N for ADF and 3.5 g COD/g N for period I). This result highlights that S-SBR N<sub>2</sub>O emission is not negatively affected by the different selection strategies with the same operative conditions, thus leading the N-SBR to be the highest contributor to direct GHG emission.

When a lower C/N ratio is adopted in period II (2 g COD/g N), while no significant deviations for influent nitrogen concentration were observed, N<sub>2</sub>O emission slightly increased, reaching 0.41 mg N<sub>2</sub>O-N/L and 0.22 mg N<sub>2</sub>O-N/L in the N-SBR and 0.33 mg N<sub>2</sub>O-N/L and 0.22 mg N<sub>2</sub>O-N/L in the S-SBR for gaseous and dissolved form, respectively. A significant increase in N<sub>2</sub>O emissions was observed during period III, characterized by a high influent sCOD concentration, which led to an increase in the ammonium dosage to adopt a C/N ratio of 1 g COD/g N. N<sub>2</sub>O gaseous concentrations reached 0.51 mg N<sub>2</sub>O-N/L and 0.46 mg N<sub>2</sub>O-N/L, while the dissolved concentrations accounted for 0.26 mg N<sub>2</sub>O-N/L and 0.24 mg N<sub>2</sub>O-N/L, both for N-SBR and S-SBR, respectively. This result is mainly due to the N<sub>2</sub>O production pathway during the nitrification (N-SBR) and denitrification process (S-SBR). As reported in the literature (Duan et al., 2021, 2017; Oba et al., 2022; Zhou et al., 2022), N<sub>2</sub>O is mainly produced as a by-product of the NH<sub>2</sub>OH oxidation pathway performed by AOB, which should represent the highest share of the N-SBR biomass. While the nitrifier denitrification pathway can also produce it, carried out by autotrophic AOB, which reduces to N<sub>2</sub>O, it has also been proved that during the denitrification, the N<sub>2</sub>O scavenging process acts, thus leading to an N<sub>2</sub>O sinking process (Conthe et al., 2019).

The N<sub>2</sub>O emission factor (Fig. 6b) reflects the same trend as the N<sub>2</sub>O emission, with the S-SBR contributing 20.92 % of the total N<sub>2</sub>O emission. During the first period (3.5 g COD/g N), the N-SBR emission factor accounted for 1.42 %, while it was 0.31 % for the S-SBR.

As expected, the highest emission factor (1.42 %) was obtained during the period I for the N-SBR. As reported in the literature (Tsuneda

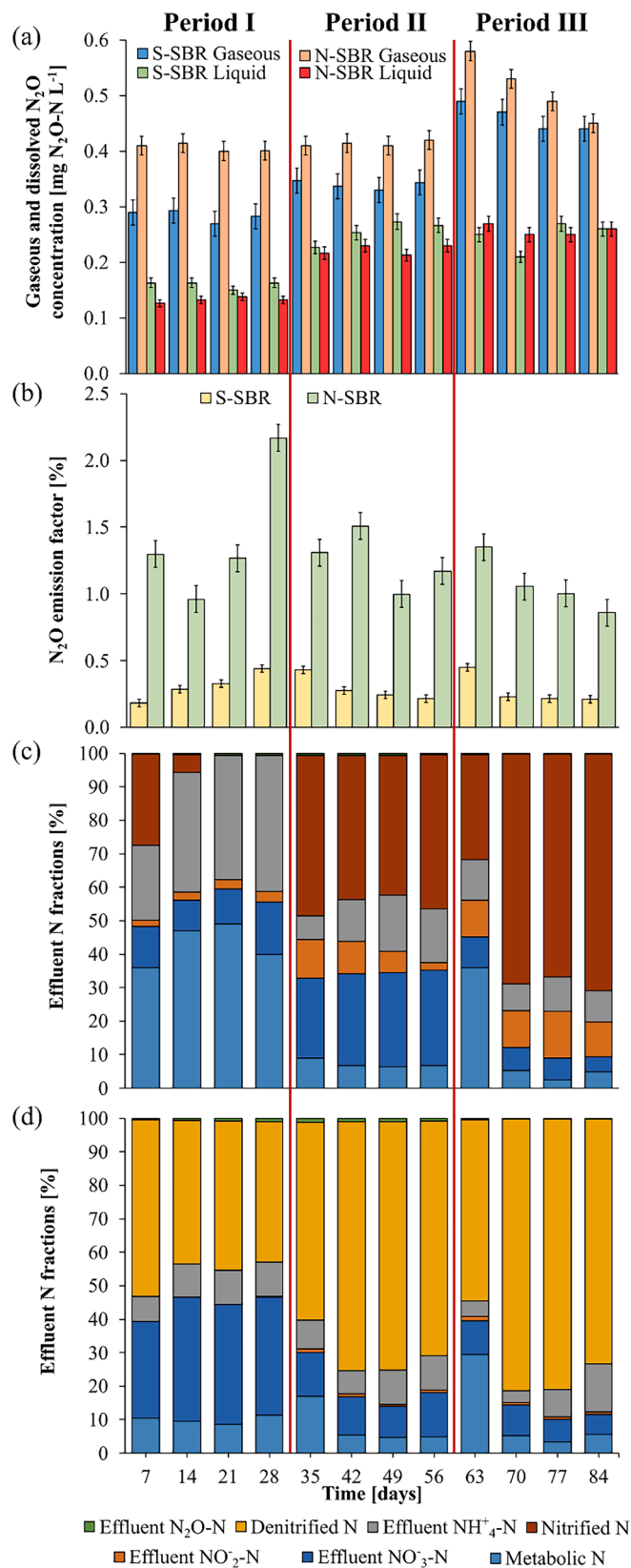


Fig. 6. Dissolved and gaseous N<sub>2</sub>O concentration for both the reactors (a), N<sub>2</sub>O emission factor for both the reactors (b), nitrogen mass balance for N-SBR (c) and S-SBR (d).



et al., 2005), the emission factor depends on the influent total nitrogen, meaning that the lower emission factor was expected during period III (C/N ratio of 1 g COD/g N) where, indeed, it reached 1.06 % for the N-SBR and 0.28 % for the S-SBR. During period II (C/N ratio of 2 g COD/g N), the N-SBR emission factor was 1.25 %, while S-SBR accounted for 0.29 %. Also, the decreasing trend reported for the N-SBR and the S-SBR during period III shows that the biomass was more able to

adapt to the stress condition of lower C/N ratio as shown by the metabolic nitrogen fractions of the influent nitrogen, reported in Fig. 6c for the N-SBR and Fig. 6d for the S-SBR.

In both cases, the first week of the last period was characterized by an increased metabolic N fraction (36.03 % for N-SBR and 29.50 % for S-SBR), with decreased nitrification/denitrification activity. Subsequently, the biomass activity was reduced to less than 5 % of

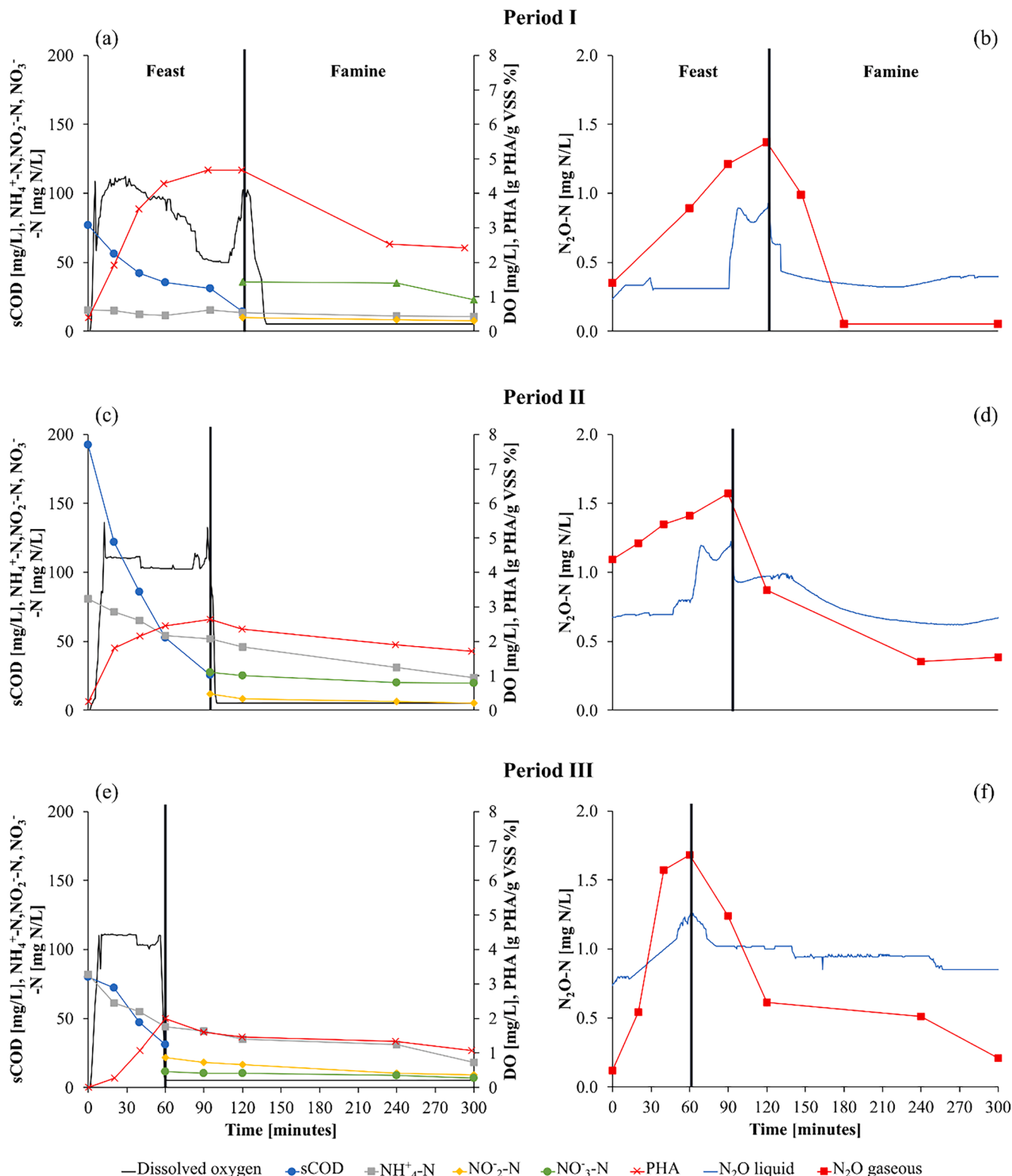


Fig. 7. Selection cycle monitoring and  $\text{N}_2\text{O}$  production in the S-SBR during periods I (a, b), II (c, d) and III (e, f).

metabolised nitrogen while autotrophic and heterotrophic activity was raised, as seen by the removal efficiencies reported in 3.2.

Fig. 7 shows the five-hour monitoring of the feast-famine cycle (Fig. 7a, c, e) coupled with the monitoring of the N<sub>2</sub>O gaseous and liquid form concentration during the feast-famine cycle (Fig. 7b, d, f) in the S-SBR for periods I, II, and III, respectively.

During the famine step, total N<sub>2</sub>O concentration (gaseous and liquid form) decreases by 20–80 % of the feast concentration, thus proving the N<sub>2</sub>O sinking during the denitrification. Moreover, it highlights the highest contribution of nitrification in N<sub>2</sub>O emission, as already shown for the N-SBR. Despite period III, characterized by an increase in influent sCOD concentration, the feast time was considerably lower (60 minutes) compared to period II (around 90 minutes) and period I (around 100 minutes). This result may be related to a more effective biomass enrichment in period III than the other periods, mainly due to the increased OLR (Table 3) (Mannina et al., 2019). As reported in the literature (Crognale et al., 2022; Isern-Cazorla et al., 2023), higher OLR enhances both biomass enrichment and PHA production while worsening the process performance. Still, despite a more successful enrichment can be deduced, a lower PHA amount was produced both during the selection (Fig. 7e) and the accumulation (Fig. 5c). As mentioned in 3.2, the amount of PHA produced is mainly influenced by the C/N ratio rather than the OLR (Basak et al., 2011; Johnson et al., 2010c). A lower C/N ratio will promote EPS production rather than PHA, thus reducing the positive effect of the OLR increase (Arshad et al., 2022; Cui et al., 2017; Zhao et al., 2021).

### 3.5. Advantages and limitations of the AE/AN enrichment

This strategy was introduced as a potential nitrogen-rich wastewater treatment coupled with biopolymer production. Indeed, one of the advantages of applying the AE/AN enrichment is the high carbon and nitrogen removal, which in this study never dropped below 80 % both in the N-SBR and S-SBR despite the C/N shifts and the high carbon and ammonia influent concentrations during period III. This result suggests the high potentiality of this strategy to achieve a high-quality effluent. Indeed, only few studies in the literature have applied this highly underexploited strategy (Conca et al., 2020; Frison et al., 2021, N. 2015b, N. 2015a). Coupling the S-SBR with advanced treatment methods, such as a membrane bioreactor, may further improve the effluent quality, thus favouring the adoption of the strategy (Traina et al., 2024). However, the high efficiency in nutrients removal is the only advantage reported. Despite the considerable amount of PHA produced, the strategy did not show an increased PHA production activity compared to the conventional ADF. It has to be said that, contrary to the other literature studies adopting this strategy, the same influent has been used for the N-SBR, S-SBR, and accumulation batch reactors in this work to mimic the strategy adoption with a nitrogen-rich carbon source. However, the results showed that the PHA production process is too sensitive towards the C/N shifts, thus suggesting that a separate nitrogen source is used only for the N-SBR operation, as N. Frison et al. (2015b) reported. Besides the amount of PHA produced, an easy-to-solve problem for this scheme, the strategy is affected by a more severe drawback: the high direct GHG emission. The S-SBR showed a considerably lower emission factor than those previously reported by the authors. In contrast, most of the time, the N-SBR's emission factor was higher than 1 % of the total influent nitrogen (Mannina and Mineo, 2024, 2023). These results also highlight the potential harmful effects of this strategy. In view of optimizing the process, future studies should first focus on understanding the mechanisms involved in N<sub>2</sub>O production in the N-SBR operation to confirm the NH<sub>2</sub>OH pathway. Afterwards, some mitigation strategies must be tested and applied without disturbing the AOB activity, like the end of pipe treatments where the reactor's off-gas can be captured (Desloover et al., 2012; Duan et al., 2021).

## 4. Conclusions

This study highlights the key impact of the C/N ratio for PHA production, contaminants removal, and N<sub>2</sub>O emission in a PHA production pilot plant using an AE/AN enrichment strategy with two separate reactors. The results of the WAS fermentation revealed the potentiality of operating the main wastewater treatment line for enhanced VFA production in view of integrating the PHA production process within the WWTPs operation. Indeed, low F/M (< 0.1 kg BOD kg SS<sup>-1</sup> day<sup>-1</sup>) and high SRT (≥ 10 days) WAS produced more propionic acid (27.1 ± 8.5 % of the total VFAs) compared to a high F/M and high SRT WAS which produced more butyric acid (27.5 ± 7.9 % of the total VFAs). If confirmed by future studies, these preliminary results may suggest WWTP operating conditions guidelines in view of improving the VFA production without further pre-treatments. The lowest C/N ratio (1 g COD/g N) showed the best condition to achieve a high nitrite accumulation rate (77 %), nitrification (89 %) and denitrification (89 %) rate while maintaining sCOD and ammonium removal above 80 % and phosphate removal above 60 %. However, this condition resulted in the highest N<sub>2</sub>O emission, reaching a total concentration of 0.77 mg N<sub>2</sub>O-N/L in the N-SBR with an emission factor of 1.06 %. Despite the higher OLR, PHA production decreased by 45 % compared to the higher C/N ratio tested (3.5 g COD/g N). The results regarding the significant GHG emissions of the N-SBR will inevitably weaken the attractiveness of this enrichment strategy, which requires future optimization. However, they point out that the environmental impact of the PHA production process cannot be neglected: future pilot-scale studies should address direct and indirect GHG emissions, focusing on their mechanisms and proposing novel mitigation strategies which do not hamper the process efficiency. Also, well-known strategies like the ADF or simpler configurations like the direct accumulation should be considered in this environmental sustainability evaluation in view of providing a comprehensive comparison and promoting the full-scale application of this technology.

### CRedit authorship contribution statement

**Antonio Mineo:** Writing – review & editing, Writing – original draft, Formal analysis, Data curation, Conceptualization. **Mark M.C. van Loosdrecht:** Writing – review & editing, Visualization, Conceptualization. **Giorgio Mannina:** Writing – review & editing, Visualization, Validation, Supervision, Resources, Project administration, Methodology, Investigation, Funding acquisition, Conceptualization.

### Declaration of competing interest

The authors declare the following financial interests/personal relationships which may be considered as potential competing interests:

One of the authors is editor in Water Research - Prof. Dr. Ir. Mark van Loosdrecht. The rest of the authors declare that they have no known competing financial interests or personal relationships that could have appeared to influence the work reported in this paper.

### Acknowledgements

This work was funded by the project “Achieving wider uptake of water-smart solutions—WIDER UPTAKE” (grant agreement number: 869283) financed by the European Union's Horizon 2020 Research and Innovation Programme, in which the last author of this paper, Giorgio Mannina, is the principal investigator for the University of Palermo. The Unipa project website can be found at: <https://wideruptake.unipa.it/>.

### Data availability

The data that has been used is confidential.

## References

- Albuquerque, M.G.E., Carvalho, G., Kragelund, C., Silva, A.F., Barreto Crespo, M.T., Reis, M.A.M., Nielsen, P.H., 2013. Link between microbial composition and carbon substrate-uptake preferences in a PHA-storing community. *ISME J.* 7, 1–12. <https://doi.org/10.1038/ismej.2012.74>.
- Albuquerque, M.G.E., Martino, V., Pollet, E., Avérous, L., Reis, M.A.M., 2011. Mixed culture polyhydroxyalkanoate (PHA) production from volatile fatty acid (VFA)-rich streams: effect of substrate composition and feeding regime on PHA productivity, composition and properties. *J. Biotechnol.* 151, 66–76. <https://doi.org/10.1016/j.jbiotec.2010.10.070>.
- Arshad, Z., Shin, K.H., Bae, H., Hur, J., 2022. Using a stable isotope tracing technique to elucidate the effect of substrate C/N ratio on the formation of different constituents of extracellular polymeric substances in an aerobic-anoxic sequencing batch reactor. *J. Water Process Eng.* 50. <https://doi.org/10.1016/j.jwpe.2022.103262>.
- Basak, B., Ince, O., Artan, N., Yagci, N., Ince, B.K., 2011. Effect of nitrogen limitation on enrichment of activated sludge for PHA production. *Bioprocess. Biosyst. Eng.* 34, 1007–1016. <https://doi.org/10.1007/s00449-011-0551-x>.
- Basset, N., Katsou, E., Frison, N., Malamis, S., Dosta, J., Fatone, F., 2016. Integrating the selection of PHA storing biomass and nitrogen removal via nitrite in the main wastewater treatment line. *Bioresour. Technol.* 200, 820–829. <https://doi.org/10.1016/j.biortech.2015.10.063>.
- Bengtsson, S., Werker, A., Visser, C., Korving, L., 2017. PHARIO: Stepping Stone to a Sustainable Value Chain For PHA Bioplastic Using Municipal Activated Sludge. *Stichting Toegepast Onderzoek Waterbeheer Amersfoort, The Netherlands*.
- Bugnicourt, E., Cinelli, P., Lazzeri, A., Alvarez, V., 2014. Polyhydroxyalkanoate (PHA): Review of synthesis, characteristics, processing and potential applications in packaging. *Express Polym. Lett.* 8, 791–808. <https://doi.org/10.3144/expresspolymlett.2014.82>.
- Chen, Yuexi, Zhang, X., Chen, Yinguang, 2021. Propionic acid-rich fermentation (PARF) production from organic wastes: a review. *Bioresour. Technol.* 339, 125569. <https://doi.org/10.1016/j.biortech.2021.125569>.
- Chen, Y.Y., Ju, S.P., Lee, D.J., 2016. Aerobic granulation of protein-rich granules from nitrogen-lean wastewaters. *Bioresour. Technol.* 218, 469–475. <https://doi.org/10.1016/j.biortech.2016.06.120>.
- Conca, V., da Ros, C., Valentino, F., Eusebi, A.L., Frison, N., Fatone, F., 2020. Long-term validation of polyhydroxyalkanoates production potential from the sidestream of municipal wastewater treatment plant at pilot scale. *Chem. Eng. J.* 390, 124627. <https://doi.org/10.1016/j.cej.2020.124627>.
- Conthe, M., Lycus, P., Arntzen, M., Ramos da Silva, A., Frostegård, Å., Bakken, L.R., Kleerebezem, R., van Loosdrecht, M.C.M., 2019. Denitrification as an N<sub>2</sub>O sink. *Water Res.* 151, 381–387. <https://doi.org/10.1016/j.watres.2018.11.087>.
- Cosenza, A., Di Bella, G., Mannina, G., Torregrossa, M., 2013. The role of EPS in fouling and foaming phenomena for a membrane bioreactor. *Bioresour. Technol.* 147, 184–192. <https://doi.org/10.1016/j.biortech.2013.08.026>.
- Crognale, S., Lorini, L., Valentino, F., Villano, M., Cristina, M.G., Barbara, T., Majone, M., Rossetti, S., 2022. Effect of the organic loading rate on the PHA-storing microbiome in sequencing batch reactors operated with uncoupled carbon and nitrogen feeding. *Sci. Total Environ.* 825, 153995. <https://doi.org/10.1016/j.scitotenv.2022.153995>.
- Cui, Y.W., Shi, Y.P., Gong, X.Y., 2017. Effects of C/N in the substrate on the simultaneous production of polyhydroxyalkanoates and extracellular polymeric substances by *Haloferax mediterranei* via kinetic model analysis. *RSC Adv.* 7, 18953–18961. <https://doi.org/10.1039/c7ra02131c>.
- Desloover, J., Vlaeminck, S.E., Clauwaert, P., Verstraete, W., Boon, N., 2012. Strategies to mitigate N<sub>2</sub>O emissions from biological nitrogen removal systems. *Curr. Opin. Biotechnol.* 23, 474–482. <https://doi.org/10.1016/j.copbio.2011.12.030>.
- Duan, H., Ye, L., Erler, D., Ni, B.J., Yuan, Z., 2017. Quantifying nitrous oxide production pathways in wastewater treatment systems using isotope technology – a critical review. *Water Res.* <https://doi.org/10.1016/j.watres.2017.05.054>.
- Duan, H., Zhao, Y., Koch, K., Wells, G.F., Zheng, M., Yuan, Z., Ye, L., 2021. Insights into nitrous oxide mitigation strategies in wastewater treatment and challenges for wider implementation. *Environ. Sci. Technol.* <https://doi.org/10.1021/acs.est.1c00840>.
- DuBois, Michel., Gilles, K.A., Hamilton, J.K., Rebers, P.A., Smith, Fred., 1956. Colorimetric method for determination of sugars and related substances. *Anal. Chem.* 28, 350–356. <https://doi.org/10.1021/ac60111a017>.
- Frigon, D., Muyzer, G., Van Loosdrecht, M., Raskin, L., 2006. rRNA and poly-β-hydroxybutyrate dynamics in bioreactors subjected to feast and famine cycles. *Appl. Environ. Microb.* 72, 2322–2330. <https://doi.org/10.1128/AEM.72.4.2322-2330.2006>.
- Frison, N., Andreolli, M., Botturi, A., Lampis, S., Fatone, F., 2021. Effects of the sludge retention time and carbon source on polyhydroxyalkanoate-storing biomass selection under aerobic-feast and anoxic-famine conditions. *ACS Sustain. Chem. Eng.* 9, 9455–9464. <https://doi.org/10.1021/acsschemeng.1c02973>.
- Frison, N., Katsou, E., Malamis, S., Oehmen, A., Fatone, F., 2015a. Development of a novel process integrating the treatment of sludge reject water and the production of Polyhydroxyalkanoates (PHAs). *Environ. Sci. Technol.* 49, 10877–10885. <https://doi.org/10.1021/acs.est.5b01776>.
- Frison, N., Katsou, E., Malamis, S., Oehmen, A., Fatone, F., 2015b. Nutrient removal via nitrite from reject water and polyhydroxyalkanoate (PHA) storage during nitrifying conditions. *J. Chem. Technol. Biotechnol.* 90, 1802–1810. <https://doi.org/10.1002/jctb.4487>.
- Fu, Z., Yang, F., Zhou, F., Xue, Y., 2009. Control of COD/N ratio for nutrient removal in a modified membrane bioreactor (MBR) treating high strength wastewater. *Bioresour. Technol.* 100, 136–141. <https://doi.org/10.1016/j.biortech.2008.06.006>.
- Geyik, A.G., Çeçen, F., 2015. Variations in extracellular polymeric substances (EPS) during adaptation of activated sludges to new feeding conditions. *Int. Biodeterior. Biodegradation* 105, 137–145. <https://doi.org/10.1016/j.ibiod.2015.08.021>.
- Gruber, W., von Känel, L., Vogt, L., Luck, M., Bionley, L., Feller, K., Moosmann, A., Krähenbühl, N., Kipf, M., Loosli, R., Vogel, M., Morgenroth, E., Braun, D., Joss, A., 2021. Estimation of countrywide N<sub>2</sub>O emissions from wastewater treatment in Switzerland using long-term monitoring data. *Water Res.* X 13. <https://doi.org/10.1016/j.wroa.2021.100122>.
- Guleria, S., Singh, H., Sharma, V., Bhardwaj, N., Arya, S.K., Puri, S., Khatri, M., 2022. Polyhydroxyalkanoates production from domestic waste feedstock: A sustainable approach towards bio-economy. *J. Clean. Prod.* <https://doi.org/10.1016/j.jclepro.2022.130661>.
- Huang, L., Jin, Y., Zhou, D., Liu, L., Huang, S., Zhao, Y., Chen, Y., 2022. A review of the role of extracellular polymeric substances (EPS) in wastewater treatment systems. *Int. J. Environ. Res. Public Health.* <https://doi.org/10.3390/ijerph191912191>.
- Isern-Cazorla, L., Mineo, A., Suárez-Ojeda, M.E., Mannina, G., 2023. Effect of organic loading rate on the production of Polyhydroxyalkanoates from sewage sludge. *J. Environ. Manage.* 343, 118272. <https://doi.org/10.1016/j.jenvman.2023.118272>.
- Jab Chung, Y., Joon Cha, H., Yeo, S., Yoo, Y.J., 1997. Production of poly(3-hydroxybutyric-co-3-hydroxyvaleric)acid using propionic acid by pH regulation. *J. Ferment. Bioeng.*
- Jelmer, T., Michel, M., Henk, D., René, R., M, van L., Mark, C., Robbert, K., 2018. Pilot-Scale polyhydroxyalkanoate production from paper mill wastewater: process characteristics and identification of bottlenecks for full-scale implementation. *J. Environ. Eng.* 144, 04018107. [https://doi.org/10.1061/\(ASCE\)EE.1943-7870.0001444](https://doi.org/10.1061/(ASCE)EE.1943-7870.0001444).
- Johnson, K., Jiang, Y., Kleerebezem, R., Muyzer, G., Van Loosdrecht, M.C.M., 2009. Enrichment of a mixed bacterial culture with a high polyhydroxyalkanoate storage capacity. *Biomacromolecules.* American Chemical Society, pp. 670–676. <https://doi.org/10.1021/bm8013796>.
- Johnson, K., Kleerebezem, R., van Loosdrecht, M.C.M., 2010a. Influence of the C/N ratio on the performance of polyhydroxybutyrate (PHB) producing sequencing batch reactors at short SRTs. *Water Res.* 44, 2141–2152. <https://doi.org/10.1016/j.watres.2009.12.031>.
- Johnson, K., Kleerebezem, R., van Loosdrecht, M.C.M., 2010b. Influence of ammonium on the accumulation of polyhydroxybutyrate (PHB) in aerobic open mixed cultures. *J. Biotechnol.* 147, 73–79. <https://doi.org/10.1016/j.jbiotec.2010.02.003>.
- Johnson, K., Kleerebezem, R., van Loosdrecht, M.C.M., 2010c. Influence of the C/N ratio on the performance of polyhydroxybutyrate (PHB) producing sequencing batch reactors at short SRTs. *Water Res.* 44, 2141–2152. <https://doi.org/10.1016/j.watres.2009.12.031>.
- Kourmentza, C., Plácido, J., Venetsaneas, N., Burniol-Figols, A., Varrone, C., Gavala, H. N., Reis, M.A.M., 2017. Recent advances and challenges towards sustainable polyhydroxyalkanoate (PHA) production. *Bioengineering.* <https://doi.org/10.3390/bioengineering4020055>.
- Kowal, P., Mehriani, M.J., Sobotka, D., Ciesielski, S., Mąkinia, J., 2022. Rearrangements of the nitrifiers population in an activated sludge system under decreasing solids retention times. *Environ. Res.* 214. <https://doi.org/10.1016/j.envres.2022.113753>.
- Li, X., Yu, Z., Ge, X., Zhang, W., Fang, Y., Liu, W., Wang, A., 2023. Volatile fatty acids bio-production using extracellular polymeric substances disengaged from sludge for carbon source recycling. *Bioresour. Technol.* 386. <https://doi.org/10.1016/j.biortech.2023.129565>.
- Liu, B., Wen, Q., Huang, L., Chen, Z., Lin, X., Liu, S., 2023. Insights into integration of polyhydroxyalkanoates (PHAs) production into wastewater treatment: Comparison of different electron acceptors on system function and PHA-producer enrichment. *Chem. Eng. J.* 451. <https://doi.org/10.1016/j.cej.2022.138631>.
- Lowry, Oliver H., Rosebrough, Nira J., Farr, A.L., Randall, Rose J., 1951. Protein measurement with the folin phenol reagent. *J. Biol. Chem.* 193, 265–275. [https://doi.org/10.1016/S0021-9258\(19\)52451-6](https://doi.org/10.1016/S0021-9258(19)52451-6).
- Mannina, G., Alduina, R., Badalucco, L., Barbara, L., Capri, F.C., Cosenza, A., Di Trapani, D., Gallo, G., Laudicina, V.A., Muscarella, S.M., Presti, D., 2021. Water resource recovery facilities (WRRFs): THE case study of palermo university (Italy). *Water* 13. <https://doi.org/10.3390/w13233413>.
- Mannina, G., Capodici, M., Cosenza, A., Di Trapani, D., 2016a. Carbon and nutrient biological removal in a University of Cape Town membrane bioreactor: Analysis of a pilot plant operated under two different C/N ratios. *Chem. Eng. J.* 296, 289–299. <https://doi.org/10.1016/j.cej.2016.03.114>.
- Mannina, G., Capodici, M., Cosenza, A., Di Trapani, D., Ekama, G.A., 2018a. Solids and hydraulic retention time effect on N<sub>2</sub>O emission from moving-bed membrane bioreactors. *Chem. Eng. Technol.* 41, 1294–1304. <https://doi.org/10.1002/ceat.201700377>.
- Mannina, G., Cosenza, A., Di Trapani, D., Capodici, M., Viviani, G., 2016b. Membrane bioreactors for treatment of saline wastewater contaminated by hydrocarbons (diesel fuel): an experimental pilot plant case study. *Chem. Eng. J.* 291, 269–278. <https://doi.org/10.1016/j.cej.2016.01.107>.
- Mannina, G., Ekama, G.A., Capodici, M., Cosenza, A., Di Trapani, D., Ødegaard, H., van Loosdrecht, M.C.M., 2018b. Influence of carbon to nitrogen ratio on nitrous oxide emission in an integrated fixed film activated sludge membrane BioReactor plant. *J. Clean. Prod.* 176, 1078–1090. <https://doi.org/10.1016/j.jclepro.2017.11.222>.
- Mannina, G., Mineo, A., 2024. A comprehensive comparison between two strategies to produce polyhydroxyalkanoates from domestic sewage sludge. *J. Clean. Prod.* 468, 143052. <https://doi.org/10.1016/j.jclepro.2024.143052>.
- Mannina, G., Mineo, A., 2023. Polyhydroxyalkanoate production from fermentation of domestic sewage sludge monitoring greenhouse gas emissions: a pilot plant case study at the WRRF of Palermo University (Italy). *J. Environ. Manage.* 348, 119423. <https://doi.org/10.1016/j.jenvman.2023.119423>.

- Mannina, G., Presti, D., Montiel-Jarillo, G., Carrera, J., Suárez-Ojeda, M.E., 2020. Recovery of polyhydroxyalkanoates (PHAs) from wastewater: a review. *Bioresour. Technol.* <https://doi.org/10.1016/j.biortech.2019.122478>.
- Mannina, G., Presti, D., Montiel-Jarillo, G., Suárez-Ojeda, M.E., 2019. Bioplastic recovery from wastewater: a new protocol for polyhydroxyalkanoates (PHA) extraction from mixed microbial cultures. *Bioresour. Technol.* 282, 361–369. <https://doi.org/10.1016/j.biortech.2019.03.037>.
- Mineo, A., Isern-Cazorla, L., Rizzo, C., Piccionello, A.P., Suárez-Ojeda, M.E., Mannina, G., 2023. Polyhydroxyalkanoates production by an advanced food-on-demand strategy: the effect of operational conditions. *Chem. Eng. J.* 472. <https://doi.org/10.1016/j.cej.2023.145007>.
- Montiel-Jarillo, G., Gea, T., Artola, A., Fuentes, J., Carrera, J., Suárez-Ojeda, M.E., 2021. Towards PHA production from wastes: the bioconversion potential of different activated sludge and food industry wastes into VFAs through acidogenic fermentation. *Waste Biomass Valorization* 12, 6861–6873. <https://doi.org/10.1007/s12649-021-01480-4>.
- Mulkerrins, D., Dobson, A.D.W., Collier, E., 2004. Parameters affecting biological phosphate removal from wastewaters. *Environ. Int.* [https://doi.org/10.1016/S0160-4120\(03\)00177-6](https://doi.org/10.1016/S0160-4120(03)00177-6).
- Oba, K., Suenaga, T., Kuroiwa, M., Riya, S., Terada, A., 2022. Exploring the functions of efficient canonical denitrifying bacteria as N<sub>2</sub>O sinks: implications from 15N tracer and transcriptome analyses. *Environ. Sci. Technol.* 56, 11694–11706. <https://doi.org/10.1021/acs.est.2c02119>.
- Puyol, D., Batstone, D.J., Hülsen, T., Astals, S., Peces, M., Krömer, J.O., 2017. Resource recovery from wastewater by biological technologies: opportunities, challenges, and prospects. *Front. Microbiol.* 7. <https://doi.org/10.3389/fmicb.2016.02106>.
- Reis, M.A.M., Serafim, L.S., Lemos, P.C., Ramos, A.M., Aguiar, F.R., Van Loosdrecht, M.C.M., 2003. Production of polyhydroxyalkanoates by mixed microbial cultures. *Bioprocess. Biosyst. Eng.* 25, 377–385. <https://doi.org/10.1007/s00449-003-0322-4>.
- Rice, E.W., Bridgewater, Laura., American Public Health Association., American Water Works Association., Water Environment Federation., 2012. *Standard Methods For the Examination of Water and Wastewater*. American Public Health Association.
- Rodríguez-Caballero, A., Aymerich, I., Marques, R., Poch, M., Pijuan, M., 2015. Minimizing N<sub>2</sub>O emissions and carbon footprint on a full-scale activated sludge sequencing batch reactor. *Water Res.* 71, 1–10. <https://doi.org/10.1016/j.watres.2014.12.032>.
- Sabapathy, P.C., Devaraj, S., Meixner, K., Anburajan, P., Kathirvel, P., Ravikumar, Y., Zbed, H.M., Qi, X., 2020. Recent developments in Polyhydroxyalkanoates (PHAs) production – a review. *Bioresour. Technol.* 306, 123132. <https://doi.org/10.1016/j.biortech.2020.123132>.
- She, Y., Hong, J., Zhang, Q., Chen, B.Y., Wei, W., Xin, X., 2020. Revealing microbial mechanism associated with volatile fatty acids production in anaerobic acidogenesis of waste activated sludge enhanced by freezing/thawing pretreatment. *Bioresour. Technol.* 302. <https://doi.org/10.1016/j.biortech.2020.122869>.
- Symons, G.E., Morey, B., 1941. The effect of drying time on the determination of solids in sewage and sewage sludges. *Sewage Work J.* 13, 936–939.
- Traina, F., Corsino, S.F., Capodici, M., Licitra, E., Di Bella, G., Torregrossa, M., Viviani, G., 2024. Combined recovery of polyhydroxyalkanoates and reclaimed water in the mainstream of a WWTP for agro-food industrial wastewater valorisation by membrane bioreactor technology. *J. Environ. Manage.* 351. <https://doi.org/10.1016/j.jenvman.2023.119836>.
- Tsuneda, S., Mikami, M., Kimochi, Y., Hirata, A., 2005. Effect of salinity on nitrous oxide emission in the biological nitrogen removal process for industrial wastewater. *J. Hazard. Mater.* 119, 93–98. <https://doi.org/10.1016/j.jhazmat.2004.10.025>.
- Ucisik, A.S., Henze, M., 2008. Biological hydrolysis and acidification of sludge under anaerobic conditions: the effect of sludge type and origin on the production and composition of volatile fatty acids. *Water Res.* 42, 3729–3738. <https://doi.org/10.1016/j.watres.2008.06.010>.
- Valentino, F., Morgan-Sagastume, F., Campanari, S., Villano, M., Werker, A., Majone, M., 2017. Carbon recovery from wastewater through bioconversion into biodegradable polymers. *N Biotechnol.* <https://doi.org/10.1016/j.nbt.2016.05.007>.
- Valentino, F., Morgan-Sagastume, F., Fraraccio, S., Corsi, G., Zanaroli, G., Werker, A., Majone, M., 2015. Sludge minimization in municipal wastewater treatment by polyhydroxyalkanoate (PHA) production. *Environ. Sci. Pollut. Res.* 22, 7281–7294. <https://doi.org/10.1007/s11356-014-3268-y>.
- Varghese, V.K., Poddar, B.J., Shah, M.P., Purohit, H.J., Khardenavis, A.A., 2022. A comprehensive review on current status and future perspectives of microbial volatile fatty acids production as platform chemicals. *Sci. Total Environ.* <https://doi.org/10.1016/j.scitotenv.2021.152500>.
- Wang, H., Chen, N., Feng, C., Deng, Y., 2021. Insights into heterotrophic denitrification diversity in wastewater treatment systems: progress and future prospects based on different carbon sources. *Sci. Total Environ.* <https://doi.org/10.1016/j.scitotenv.2021.146521>.
- Wu, M., Liu, X., Tu, W., Xia, J., Zou, Y., Gong, X., Yu, P., Huang, W.E., Wang, H., 2023. Deep insight into oriented propionate production from food waste: Microbiological interpretation and design practice. *Water Res.* 243. <https://doi.org/10.1016/j.watres.2023.120399>.
- Yang, F., Huang, J., Xu, S., Huang, X., Guo, J., Fang, F., Chen, Y., Yan, P., 2022. Influence of nitrogen-poor wastewater on activated sludge aggregation and settling: Sequential responses of extracellular proteins and exopolysaccharides. *J. Clean. Prod.* 359. <https://doi.org/10.1016/j.jclepro.2022.132160>.
- Ye, M., Ye, J., Luo, J., Zhang, S., Li, Y.Y., Liu, J., 2020. Low-alkaline fermentation for efficient short-chain fatty acids production from waste activated sludge by enhancing endogenous free ammonia. *J. Clean. Prod.* 275. <https://doi.org/10.1016/j.jclepro.2020.122921>.
- Zhang, C., Chen, Y., 2009. Simultaneous nitrogen and phosphorus recovery from sludge-fermentation liquid mixture and application of the fermentation liquid to enhance municipal wastewater biological nutrient removal. *Environ. Sci. Technol.* 43, 6164–6170. <https://doi.org/10.1021/es9005948>.
- Zhao, L., Bao, M., Zhao, D., Li, F., 2021. Correlation between polyhydroxyalkanoates and extracellular polymeric substances in the activated sludge biosystems with different carbon to nitrogen ratio. *Biochem. Eng. J.* 176. <https://doi.org/10.1016/j.bej.2021.108204>.
- Zhou, Y., Zhao, S., Suenaga, T., Kuroiwa, M., Riya, S., Terada, A., 2022. Nitrous oxide-sink capability of denitrifying bacteria impacted by nitrite and pH. *Chem. Eng. J.* 428. <https://doi.org/10.1016/j.cej.2021.132402>.